ELSEVIER

Biochimica et Biophysica Acta 1512 (2001) 77–89

BIOCHIMICA ET BIOPHYSICA ACTA
BBA

www.bba-direct.com

Interaction and structure induction of cell-penetrating peptides in the presence of phospholipid vesicles

Mazin Magzoub [a], Kalle Kilk [1,b], L.E. Göran Eriksson [a], Ülo Langel [2,b], Astrid Gräslund [a,*]

[a] *Department of Biochemistry and Biophysics, Arrhenius Laboratories, Stockholm University, S-106 91 Stockholm, Sweden*
[b] *Department of Neurochemistry and Neurotoxicology, Arrhenius Laboratories, Stockholm University, S-106 91 Stockholm, Sweden*

Received 3 January 2001; received in revised form 22 February 2001; accepted 28 February 2001

Abstract

Certain short peptides, which are able to translocate across cell membranes with a low lytic activity, can be useful as carriers (vectors) for hydrophilic molecules. We have studied three such cell penetrating peptides: pAntp ('penetratin'), pIsl and transportan. pAntp and pIsl originate from the third helix of homeodomain proteins (Antennapedia and Isl-1, respectively). Transportan is a synthetic chimera (galanin and mastoparan). The peptides in the presence of various phospholipid vesicles (neutral and charged) and SDS micelles have been characterized by spectroscopic methods (fluorescence, EPR and CD). The dynamics of pAntp were monitored using an N-terminal spin label. In aqueous solution, the CD spectra of the three peptides show secondary structures dominated by random coil. With phospholipid vesicles, neutral as well as negatively charged, transportan gives up to 60% α-helix. pAntp and pIsl bind significantly only to negatively charged vesicles with an induction of around 60% β-sheet-like secondary structure. With all three peptides, SDS micelles stabilize a high degree of α-helical structure. We conclude that the exact nature of any secondary structure induced by the membrane model systems is not directly correlated with the common transport property of these translocating peptides.

Keywords: Homeo-peptide; Penetratin; Transportan; Phospholipid vesicle; Interaction; Secondary structure

1. Introduction

A number of natural and synthetic peptides, soluble in water, are able to translocate various cell membranes non-endocytically and are defined as cell penetrating peptides (CPPs) [1,2]. Of particular interest

Abbreviations: pAntp, penetratin, Antennapedia homeodomain derived transport peptide; pIsl, Isl-1 homeodomain derived transport peptide; CD, circular dichroism; CPP, cell penetrating peptide; EPR, electron paramagnetic resonance; DMPC, dimyristoylphosphatidylcholine; DOPC, dioleoylphosphatidylcholine; DMPG, dimyristoylphosphatidylglycerol; DOPG, dioleoylphosphatidylglycerol; PS, phosphatidylserine; SDS, sodium dodecyl sulfate; HFP, hexafluoroisopropanol; MTS-SL, spin label (1-oxyl-2,2,5,5-tetramethylpyrroline-3-methyl) methanethiosulfonate; FTIR, Fourier transform infrared spectroscopy

* Corresponding author. Fax: +46-8-155-597; E-mail: astrid@dbb.su.se

[1] On leave from Department of Biochemistry, University of Tartu, Ravila 19, 50411 Tartu, Estonia. Present address: Department of Neuropharmacology, Harold L. Dorris Neurological Research Center, Scripps Research Institute, La Jolla, CA 92037, USA.

[2] Present address: Department of Neuropharmacology, Harold L. Dorris Neurological Research Center, Scripps Research Institute, La Jolla, CA 92037, USA.

0005-2736/01/$ – see front matter
PII: S0005-2736(01)00304-2

are those peptides which have low lytic activity. These translocating peptides, also known as Trojan peptides [1], have been applied as vectors for the delivery of hydrophilic biomolecules and drugs into cytoplasmic and nuclear compartments of cells, both in vivo and in vitro [1,2]. When covalently linked with a 'cargo', including polypeptides and oligonucleotides with many times their own molecular mass, these peptides are still able to translocate. This finding has even allowed antisense regulation experiments in rat, in vivo [3] and in cultured rat neurons [4].

Examples of useful transport peptides are sequences derived from homeodomains of certain transcription factors, as well as so-called Tat-derived peptides and peptides based on signal sequences. Purely synthetic or chimeric peptides have also been designed, as reviewed in [1,2]. Homeodomain (homeobox) proteins belong to a class of transcription factors involved in multiple morphological processes [5]. The first of the homeodomain-derived translocating peptides was 'penetratin', denoted pAntp, with a sequence corresponding to the 16 residues of the third α-helix (residues 43–58) from the Antennapedia homeodomain protein of *Drosophila* [6–8]. This third helix was found to be responsible for the translocation of the entire protein [7]. The pAntp peptide alone retains its membrane translocation properties and has therefore been proposed as a universal intercellular delivery vector [1].

For nuclear import, in general, it has been found that the signal sequence contains some positively charged (basic) residues [2]. It seems that such charged amino acids are also required for plasma membrane translocation. It has also been found that for certain types of CPPs, cellular internalization occurs at 37°C as well as 4°C and cannot be saturated [1,2,7,8]. The internalization does not require a chiral receptor protein, since enantiomeric discrimination is not observed [1,7].

Nevertheless, the complete mechanisms of translocation for the different CPPs are still mostly unknown. For instance, it is not known whether any particular secondary structure has to be induced in order to allow (energetically) a translocation, involving a concomitant transient membrane destabilization. It is clear, however, that the molecular details of the peptide-membrane interactions must be of fundamental importance for the translocation process. The present study aims at an understanding of these interactions in various membrane mimetic model systems.

We have studied three membrane translocating peptides (Fig. 1). One is 'transportan', a synthetic chimera with good vectorial properties. Transportan is a product of fusion between an N-terminal fragment from the neuropeptide galanin and the mastoparan peptide (originating from wasp venom) with an extra Lys residue inserted between the two fused sequences [9]. The other two CCPs are homeodomain-derived peptides: pAntp and pIsl. The latter peptide was selected from the third helix (residues 45–60) of the homeodomain of the transcription factor Islet-1 (Isl-1), which belongs to the LIM family of homeodomains [10,11]. The pIsl peptide contains only a single tryptophan residue (Trp, W; cf. Fig. 1). This Trp is conserved between all the homeodomains [10]. We have recently found that pIsl functions as an efficient CPP in cellular systems (unpublished results).

The interaction of pAntp and transportan with SDS micelles has been studied by ^{1}H NMR and

Peptide	Origin	Sequence
pIsl	Isl-1 HD (LIM family)	RVIRVWFQNKRCKDKK
pAntp (penetratin)	Antennapedia HD (homeotic family)	RQIKIWFQNRRMKWKK
Transportan	Chimera (galanin-mastoparan)	GWTLNSAGYLLGKINLKALAALAKKIL

Fig. 1. The origin and amino acid sequences of the three cell penetrating peptides studied. The Trp (W) residues of the peptides are underlined.

CD [12,13]. The SDS membrane mimetic system promotes α-helical structure in pAntp. For transportan, SDS micelles were found to induce about 60% helical structure, located in the C-terminal mastoparan part of the sequence [12].

In the present work we use vesicles of various phospholipid compositions, uncharged and negatively charged, as model systems for the membrane interaction studies on the transport peptides. Three spectroscopic techniques are employed: fluorescence, CD and EPR, which give information on secondary structures and dynamics of the peptides in the different environments.

2. Materials and methods

2.1. Materials

Penetratin (pAntp), Cys(-1)-pAntp, pIsl and transportan (Fig. 1) were produced by Neosystem Laboratoire (Strasbourg). The identity and purity were controlled by amino acid, mass spectroscopy and HPLC analysis. Dimyristoylphosphatidylcholine (DMPC; Sigma), dioleoylphosphatidylcholine (DOPC; Avanti Polar Lipids, Alabaster), dimyristoylphosphatidylglycerol (DMPG; Larodan, Malmö), dioleoylphosphatidylglycerol (DOPG; Avanti) and phosphatidylserine (PS; sheep brain, grade 1; Lipid Products, Surrey), were all of best quality and used without further purification. The thiol-specific spin label reagent (1-oxyl-2,2,5,5-tetramethylpyrroline-3-methyl) methanethiosulfonate (MTS-SL) was purchased from Renal Factory (Budapest).

2.2. Preparation of vesicles and micelles

Phospholipid vesicles were prepared from 1 mM phospholipid in 50 mM potassium phosphate buffer (pH 7.0), using a Heat System Model 350 A Sonifier. The ice-cooled dispersion was sonicated under nitrogen until the transparency was maximized. The duration of sonication was approx. 1 h, and with the microtip at a low output control (setting 4) and 50% duty cycle. Titanium particles were removed by centrifugation. This preparation procedure results in vesicles with dimensions of less than 100 nm in diameter [14]. The micelle solution was prepared as 100 mM sodium dodecyl sulfate (SDS, from Kebo) in water, well above the critical micelle concentration. The pH of the solution was about 3.

2.3. Determination of peptide concentrations

After weighing on a microbalance the peptide concentrations in the stock solutions were determined by light absorption on a CARY 4 Spectrophotometer, using cuvettes with 2 mm light path. All the spectra were baseline corrected. A molar absorptivity of 5600 M^{-1} cm^{-1} for one Trp was used for quantitation.

2.4. Spin labeling of penetratin

5 mg of cysteine-pAntp was dissolved in a mixture of acetonitrile (200 μl) and aqueous 0.1% trifluoroacetic acid (100 μl). A 5-fold molar excess of the thiol-specific spin label reagent MTS-SL dissolved in acetonitrile (50 μl) was added. The mixture was kept at room temperature overnight. After freeze drying the product was purified by reversed HPLC on a C18 column with an acetonitrile/trifluoroacetic acid gradient.

2.5. Fluorescence

Tryptophan fluorescence was measured on a Perkin Elmer LS 50B Luminescence Spectrometer with FL WinLab software. All measurements were made in 4×10 mm cuvettes at an ambient temperature of about 20°C. The fluorescence was excited at 280 nm and the emission scanned from 300 to 500 nm. Scans were taken with a 10 nm excitation and emission bandwidth and a scan speed of 250 nm/min.

The concentration of peptides was 10 μM, also in the presence of 100 mM SDS micelles or small vesicles from 1 mM phospholipids (DOPG, DMPG and DMPC). For the Trp fluorescence quenching experiments, acrylamide was added from a 1 M stock solution, resulting in concentrations between 4 and 100 mM. For samples containing vesicles, the background signal intensity was subtracted from the spectrum of the peptide-containing sample. Quenching constants K_{SV} were determined by a linear regression with the Stern-Volmer equation for a dynamic process [15]:

$$\frac{F_0}{F} = 1 + K_{SV}[Q] \quad (1)$$

where F and F_0 are the fluorescence intensities in the presence and absence of acrylamide, respectively. [Q] is the total molar concentration of the quencher acrylamide in the solution.

2.6. EPR spectroscopy

EPR spectra were recorded on a Bruker Lexus500 spectrometer system. Each sample was drawn into a 1 mm glass capillary. This was placed within a quartz tube in the cavity, kept at room temperature (20°C). Conventional first harmonic, in-phase, absorption spectra were recorded at a modulation frequency of 100 kHz and modulation amplitude of 0.25 mT, at maximum. The spectra were collected over a range of 8 mT and averaged over three scans, with a sampling time of 0.3 s.

The rotational correlation time, τ_c, which gives an indication of the mobility of the spin label, was estimated using the simplified equation for rapid isotropic motion:

$$\tau_c = 6.5 \times \Delta W \left[\sqrt{\frac{h(0)}{h(-1)}} - 1 \right] \quad (2)$$

where τ_c is in nanoseconds, ΔW is the width (mT) of the central line in the X-band first derivative EPR spectrum, and $h(-1)$ and $h(0)$ are the peak-to-peak heights of the high-field and central lines, respectively [16].

2.7. Circular dichroism spectroscopy

CD measurements were made on a Jasco J-720 CD spectropolarimeter with 0.5 and 1 mm quartz cuvettes. Wavelengths from 190 to 300 nm were measured, with a 0.2 nm step resolution at 100 nm/min speed. The response time was 4 s, with 50 or 100 mdeg sensitivity and a 1 nm bandwidth. The temperature was regulated by a PTC-343 controller, usually set at 20°C. Spectra were collected and averaged over ten scans. Peptide concentrations were 10 μM. Lipid-containing samples had various concentrations of phospholipid, ranging from 100 μM to 5 mM, or 100 mM SDS. Contributions from background signals were subtracted from the CD spectra acquired for the peptides.

The amount of α-helical structure may be determined by assuming that only a random coil and an α-helix secondary structure were present. This leads to the following simplified equation [14]:

$$\%\ \alpha\text{-helix} = 100 \times (B - \Theta_\lambda)/(B - A) \quad (3)$$

where A and B are the mean residue molar ellipticities at a wavelength λ for a model α-helix and a model random coil conformation, respectively. Θ_λ is the mean residue molar ellipticity of the sample at the same wavelength. Calculations were performed using the ellipticity at 222 nm, where the contribution to ellipticity of any β-sheet component is small. At 222 nm the molar ellipticity of a random coil CD spectrum is 3900 deg cm^2 dmol^{-1}, and the α-helical contribution to ellipticity has its most negative value, −38 000 deg cm^2 dmol^{-1} [14]. In the case of another two-state situation with only a β-sheet and a random coil in equilibrium a similar approach at another wavelength may, in principle, be applied.

From such initial estimates of assumed two-component spectra, graphical fittings using reference spectra were performed to increase the overall accuracy of the estimated proportions. We started from two reference spectra, random coil and α-helix or random coil and antiparallel β-sheet [17]. The two components were then added with varying percentage weights, until a match for the recorded spectrum was obtained by visual inspection. Computer fittings using the VARSELEC program [18], with up to five reference component spectra, were also performed, but this method was found not to improve the fitting significantly and to lead to over-interpretation of the spectra.

3. Results

3.1. Fluorescence spectroscopy

3.1.1. Homeo-peptides

The intrinsic Trp fluorescence of the pAntp, pIsl and transportan peptides (sequences in Fig. 1) was studied in various media. The pAntp peptide has two Trp residues, whereas pIsl and transportan have one Trp each. The Trp fluorescence from all three pep-

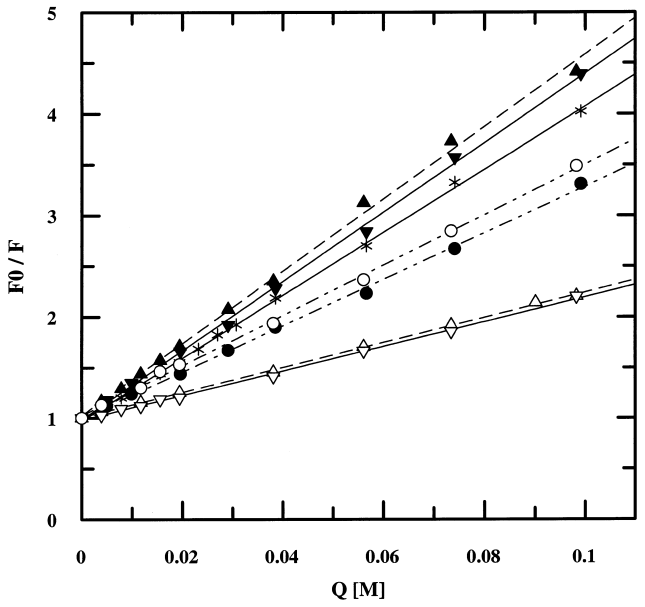

Fig. 2. Stern-Volmer plots for the acrylamide quenching of the tryptophan fluorescence from peptides in the presence of small phospholipid vesicles, composed of 1 mM DMPG (open symbols) or DMPC (filled symbols). pAntp (▽), pIsl (△) and transportan (○) were at 10 μM concentration. The plot for transportan in 50 mM phosphate buffer, pH 7.0 (*) is also shown as a reference.

tides obeys the linear Stern-Volmer equation with acrylamide as a neutral hydrophilic quencher (Fig. 2).

In aqueous buffer alone, pAntp has a peak Trp emission wavelength of about 354 nm, and a Stern-Volmer quenching constant of 35 M^{-1} (Table 1). These are the same as the values measured for monomeric (free) Trp itself in water. In the presence of neutral vesicles (DMPC) pAntp has approximately the same wavelength and quenching constant as in water, and therefore does not appear to associate with the vesicles. With the negatively charged vesicles (DMPG and DOPG), the emission peak wavelength is shifted to around 340 nm. This shift towards a shorter wavelength ('blue shift') is representative of the Trp residue being partitioned into a more hydrophobic environment [15]. The result also indicates that the Trp is only partially buried in the vesicles, since a moiety fully protected from water is expected to have its emission at about 320 nm [15]. The partial protection from the aqueous solvent is further supported by the corresponding decrease in the quenching constant to around 12 M^{-1}. It has to be noted that there is no indication from the Stern-Volmer graphs that the two Trps of pAntp (W in Fig. 1) respond differently to the quenching.

The behavior of pAntp is mirrored by pIsl with its single Trp. In water the peptide has a peak Trp emission wavelength of about 353 nm, and a quenching constant of 39 M^{-1} (Table 1). In the presence of neutral vesicles (DMPC), there is no wavelength shift and therefore, again, no evidence for binding. With DMPG and DOPG vesicles, the peak wavelengths are blue shifted to around 340 nm, and the quenching constants are reduced to around 13 M^{-1}. These results suggest that for the pAntp and pIsl the membrane association is largely charge dependent.

3.1.2. Transportan

Transportan has a Trp peak emission wavelength of 353 nm in water and a Stern-Volmer quenching constant of 31 M^{-1} (Table 1). In all phospholipid vesicles, irrespective of charge, the peak emission wavelength is shifted to 335–340 nm and a quenching constant of 23–24 M^{-1} is observed. In SDS micelles, similar values of emission peak wavelength and quenching constant as in the vesicles were observed (data not shown). The results indicate that the asso-

Table 1
Tryptophan fluorescence results for the three cell penetrating peptides

Medium	pAntp		pIsl		Transportan	
	λ_{peak} (nm)	K_{SV} (M^{-1})	λ_{peak} (nm)	K_{SV} (M^{-1})	λ_{peak} (nm)	K_{SV} (M^{-1})
Buffer (pH 7)	354	35	353	39	353	31
1 mM DMPC	354	34	353	36	340	23
1 mM DMPG	341	12	341	13	335	24
1 mM DOPG	340	14	340	16	336	24

Given are the wavelengths of peak emission, λ_{peak}, as well as the Stern-Volmer constants, K_{SV}, for the quenching with acrylamide. All measurements were made at 20°C. Excitation was at 280 nm. Peptide concentrations were 10 μM in the presence of small phospholipid vesicles prepared from 1 mM phospholipids (in 50 mM phosphate buffer, pH 7.0) by sonication.

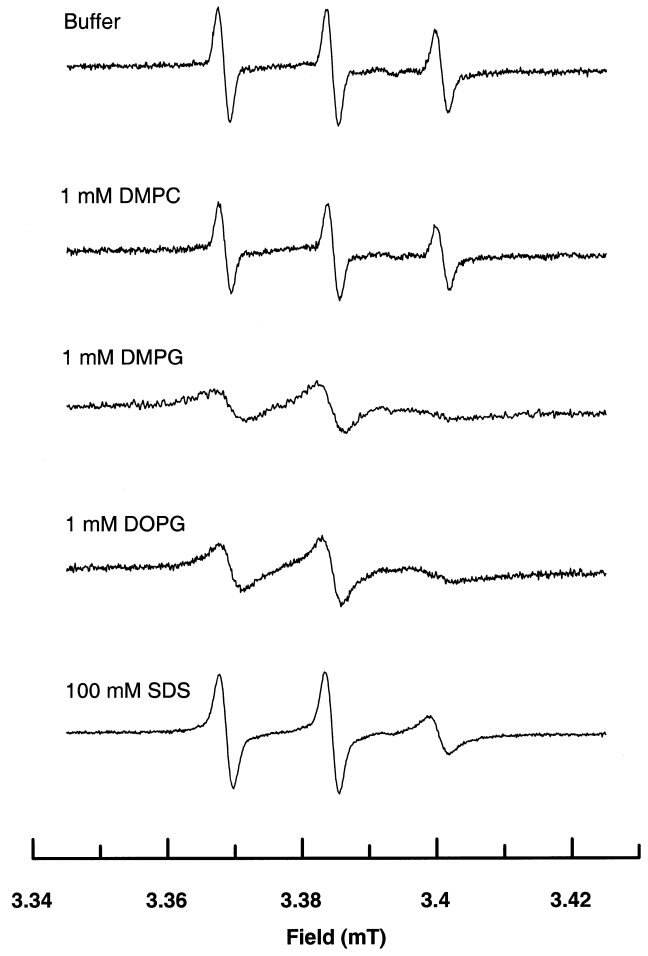

Fig. 3. EPR spectra of 10 μM Cys-pAntp, spin labeled by the MTS-SL reagent, and recorded in the presence of (from top to bottom): 50 mM phosphate buffer, pH 7.0, 1 mM DMPC, 1 mM DMPG, 1 mM DOPG vesicles in buffer, pH 7.0, and 100 mM SDS micelles in water, pH 3. The temperature was 20°C.

ciation of transportan to the membrane mimics is charge independent, and is instead governed by the potent hydrophobic properties of the mastoparan sequence in its C terminus.

3.2. Electron paramagnetic resonance spectroscopy

In order to obtain dynamic information about the interaction between pAntp and the membrane mimics, EPR spectroscopy was used to study a spin-labeled Cys(-1)-pAntp in the presence of neutral and negatively charged phospholipid vesicles as well as negatively charged SDS micelles. Spectra were recorded with 10 μM peptide in the presence of 1 mM (Fig. 3) and 0.1 mM (Fig. 4) phospholipid concentrations, as well as in the presence of 100 mM SDS (Fig. 3). Assuming rapid isotropic motion, the rotational correlation times of the spin label were estimated from the line shape of the recorded first derivative EPR spectra [16], using Eq. 2. Table 2 shows the rotational correlation times of the spin-labeled pAntp in the different membrane mimic solvents. We observe the same line shapes – and derive the same values for the correlation times of the peptide – in the presence of both the 0.1 mM and 1 mM phospholipid concentrations.

The EPR spectrum for the peptide in buffer gives three sharp peaks, which is characteristic of a freely moving spin-labeled peptide with a rotational correlation time, τ_c, of about 0.2 ns (Table 2). The spec-

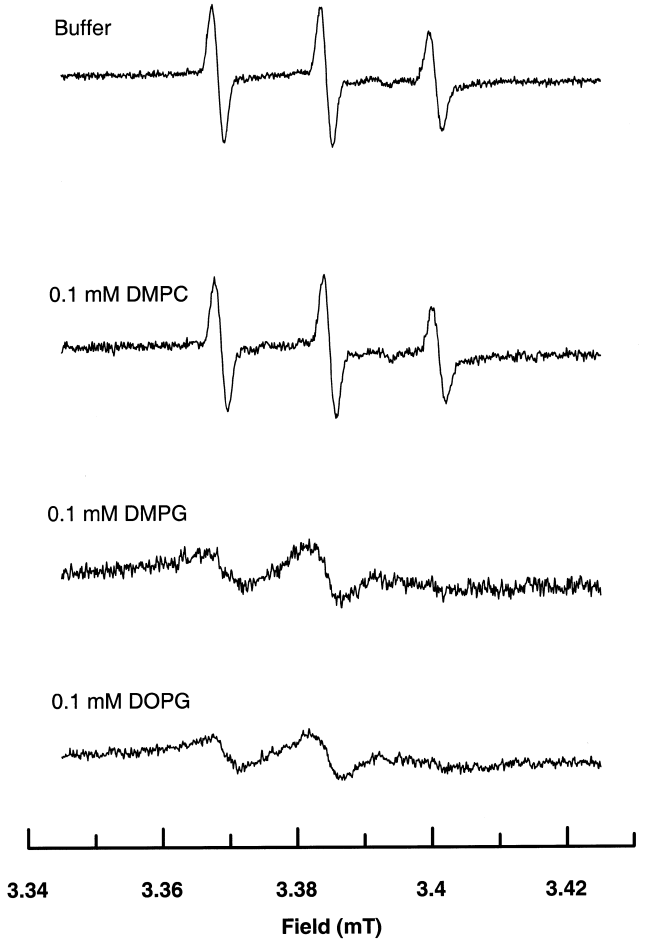

Fig. 4. EPR spectra of spin-labeled 10 μM Cys-pAntp in the presence of (from top to bottom): 50 mM phosphate buffer, pH 7.0, 0.1 mM DMPC, 0.1 mM DMPG and 0.1 mM DOPG vesicles in buffer. The temperature was 20°C.

Table 2
The rotational correlation time (τ_c, ns) determined from EPR studies of 10 μM spin-labeled Cys-pAntp in the presence of various membrane mimics: SDS micelles in water, pH 3, DMPC, DMPG and DOPG vesicles in 50 mM phosphate buffer, pH 7.0

Medium	Buffer	SDS 100 mM	DMPC		DMPG or DOPG	
			1 mM	0.1 mM	1 mM	0.1 mM
Rotational correlation time, τ_c (ns)	0.2	1.1	0.2	0.2	~2	~2

The samples were maintained at room temperature (20°C).

trum for the peptide in the presence of the neutral DMPC vesicles is very similar to that in buffer, with $\tau_c = 0.2$ ns, indicating a lack of association of the peptide with the neutral vesicles. In 100 mM SDS micelles, there is a significant broadening of the third peak, resulting in an estimated rotational correlation time of 1.1 ns. The spectrum is characteristic for the rotation of an SDS micelle alone, containing a fatty acid spin probe (5-doxylstearic acid) [19]. Hence, it reflects the restrictions imposed on the pAntp peptide by its binding to the SDS micelle. In DMPG and DOPG there is substantial broadening of all three peaks (Fig. 3), indicating a dominating association of the peptide with the negatively charged vesicles, with no significant contribution from a free component. The degree of broadening also reflects the restricted mobility of the larger vesicles, as opposed to the smaller micelles. According to Eq. 2, we estimate that $\tau_c \approx 2$ ns with the charged vesicles (DMPG and DOPG). We have to bear in mind that Eq. 2 assumes rapid motion, which is not the case with vesicles. Nevertheless, considering the much larger volume of a vesicle one would expect an even stronger immobilization, if no intrinsic mobility of the probe exists. According to the Stokes-Einstein equation we should expect a rotational correlation time τ_c value of the order of 10 ns for a peptide in an SDS micelle (approximate diameter 35 Å) at ambient temperature [20], and a much slower (three order of magnitudes) τ_c in vesicles (approximate diameter 100 nm). This indicates that the N-terminal moiety and the spin label retain considerable local mobility, particularly in the vesicles.

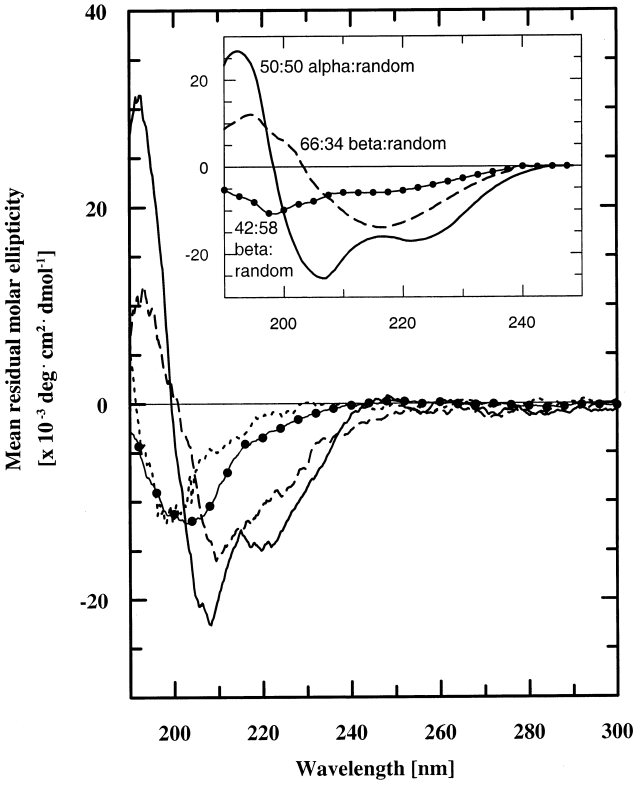

Fig. 5. CD spectra of 10 μM pAntp in the presence of 50 mM phosphate buffer, pH 7.0 (●), 100 mM SDS micelles in water, pH 3 (———), 0.1 mM DMPG vesicles (— — —), and 0.1 mM DMPC vesicles (- - -) in buffer. Insert: graphical fittings corresponding to the recorded spectra. The graphical fittings were obtained by starting from two reference spectra, random coil and α-helix or antiparallel β-sheet [17], and then adding the two components in varying percentage weightings, until a best match for the recorded spectrum was obtained by visual inspection.

3.3. Circular dichroism spectroscopy

3.3.1. Homeo-peptides

The pAntp, pIsl and transportan peptides and their association and possible structure induction by membrane mimicking solvents were studied by CD spectroscopy. Figs. 5 and 6 show the CD spectra of 10 μM pAntp and pIsl free in the buffer medium, and in the presence of the three biomembrane models (DMPC and DMPG vesicles, and SDS micelles). The temperature was 20°C for direct comparison with the

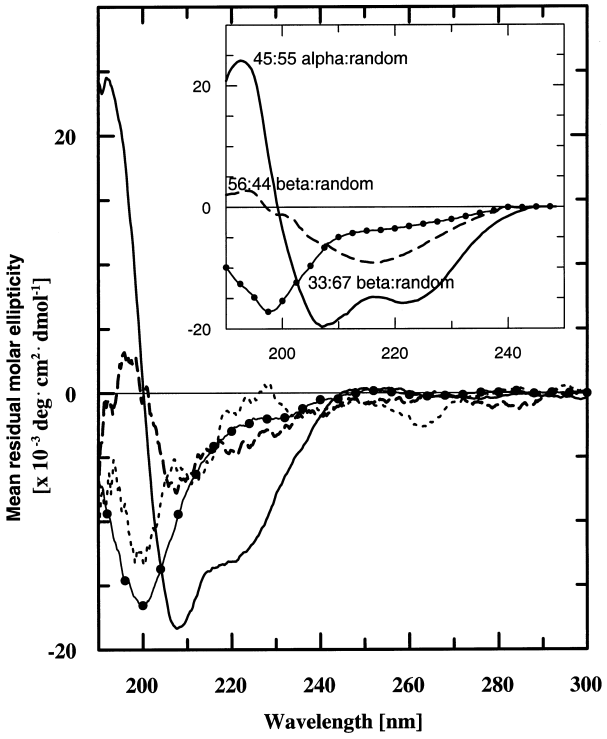

Fig. 6. CD spectra of 10 μM pIsl in the presence of 50 mM phosphate buffer, pH 7.0 (●), 100 mM SDS micelles in water, pH 3 (——), 0.1 mM DMPG vesicles (— — —), and 0.1 mM DMPC vesicles (- - -) in buffer. Insert: graphical fittings corresponding to the recorded spectra.

EPR results. Table 3 gives a summary of the structure induction results for the two homeo-peptides, further illustrating the similarities in their behavior.

CD spectroscopy revealed no dominating secondary structure component for pAntp and pIsl in aqueous buffer in the concentration range 0.01–1 mM. Also at the highest concentration of pAntp the CD spectrum indicates a mainly random coil state (spectra not shown). Analysis of CD spectral components, at 10 μM peptide concentrations, using graphical fittings (inserts, Figs. 5 and 6) gives 42% and 33% antiparallel β-sheet content in buffer for pAntp and pIsl, respectively, in addition to the random coil components. The spectra could not be fitted assuming significant α-helical contributions. We also found that the AGADIR prediction program [21] did not indicate any helical content for the homeo-peptides in aqueous solution.

In 100 mM SDS micelles a significant amount of helix structure is induced in the homeo-peptides (Figs. 5 and 6). The helicities in the micelles are 45–50% and 40–45% for pAntp and pIsl, respectively. This is about the same degree of helicity induced in mixtures of water and hexafluoropropanol (HFP), where 10% vol. HFP was found to be enough to promote a significant change of the CD spectrum (data not shown). At 30% HFP a maximal degree of helicity of around 60% is induced (spectra not shown).

Table 3
CD results for the two homeo-peptides, pAntp and pIsl

Medium	pAntp			pIsl		
	$[\theta]_{222}$ (deg cm^2 dmol^{-1})	Structure	%	$[\theta]_{222}$ (deg cm^2 dmol^{-1})	Structure	%
Buffer (pH 7)	−2 000	β-sheet (antiparallel)	42	−2 000	β-sheet (antiparallel)	33
		random coil	58		random coil	67
0.1 mM DMPC	−1 400	n.d.		−1 200	n.d.	
0.1 mM DMPG	−9 600	β-sheet (antiparallel)	66	−5 000	β-sheet (antiparallel)	56
		random coil	34		random coil	44
100 mM SDS	−15 000	α-helix	50 (45)	−13 000	α-helix	45 (40)
		random coil	50		random coil	55
HFP:H_2O (3:7)	−19 500	α-helix	56	−21 300	α-helix	60

The spectra were measured at 20°C. Peptide concentrations were 10 μM, in the presence of vesicles prepared from 0.1 mM phospholipids (in 50 mM phosphate buffer, pH 7.0), or 100 mM SDS (in water, pH 3). The mean residual molar ellipticity values at 222 nm, $[\theta]_{222}$, are shown. The α-helix and β-sheet contents were determined using a method of graphical fittings, where we started from two reference spectra, and then added the two components in varying percentage weightings, until a match for the recorded spectrum was obtained by visual inspection. Reference spectra [17] for random coil, α-helix and antiparallel β-sheet were used. The α-helix content in SDS micelles was also calculated according to Eq. 3, using the $[\theta]_{222}$ value (given in parentheses). For 0.1 mM DMPC the secondary structure components could not be determined (n.d.) due to a combination of severe light scattering and weak CD signals.

Working with vesicle samples in the CD spectrometer caused problems due to light scattering, particularly where weak CD signals were observed in the absence of a dominating helical component. A vesicle suspension was used as a blank sample and reduction of the optical length was employed. At the highest lipid concentration (5 mM) severe light scattering had to be taken care of by reducing the optical length (to 0.05 mm). With the vesicle samples containing 10 μM pAntp or pIsl we had to reduce the phospholipid concentration from 1 mM to only 0.1 mM in order to avoid severe light scattering problems. From the identical EPR spectra of spin-labeled pAntp in the presence of 0.1 mM and 1 mM phospholipid concentrations we have verified that the peptide interacts similarly with the phospholipids at both concentrations (Table 2; Figs. 3 and 4). Moreover, the CD properties of the spin-labeled pAntp were identical to those of the non-labeled compound.

With the neutral vesicles (0.1 mM DMPC) and 10 μM peptides, the apparent lack of association of the peptides is reflected in the poor structure induction effect (Figs. 5 and 6). Even at the higher lipid:peptide ratio of 100:1 the CD spectra are close to those in buffer (data not shown). We also exposed 10 μM pAntp to various concentrations of DMPC vesicles, ranging from 0.01 mM to 5 mM. The CD spectra seem to indicate a weak gradual structural stabilization upon increasing the DMPC vesicle concentration, although we are still unable to detect a dominating secondary structure component.

In the presence of 1 mM DMPG vesicles, where association was observed through fluorescence and EPR (for pAntp), a slight indication of a structure induction was observed for the 10 μM peptides. The CD spectra of pAntp in the presence of 1 mM DMPG vesicles were not significantly affected by variation of the temperature below and above the lipid gel to liquid crystal phase transition at about 23°C (data not shown). Upon reducing the phospholipid concentration to 0.1 mM, in order to reduce the light scattering problems, the CD spectra revealed a significant degree of β-sheet like contributions (Figs. 5 and 6). Graphical fittings, used to estimate the magnitude of the structural components, gave 66 and 56% antiparallel β-sheet content for pAntp and pIsl, respectively (inserts, Figs. 5 and 6).

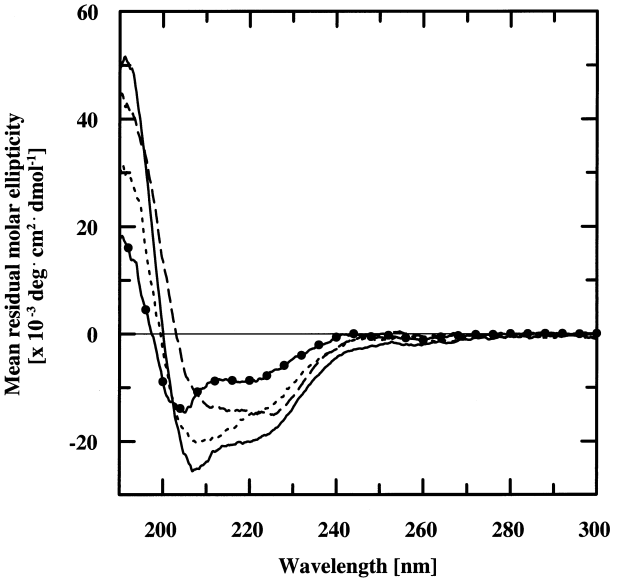

Fig. 7. CD spectra of 10 μM transportan in the presence of 50 mM phosphate buffer, pH 7.0 (●), 100 mM SDS micelles in water, pH 3 (———), 0.1 mM DMPG vesicles (— — —), and 0.1 mM DMPC vesicles (- - -) in buffer.

3.3.2. Transportan

Transportan, studied at 10 μM by CD, was found to have 30% α-helical content, in addition to random coil, in aqueous buffer (Fig. 7). The AGADIR algorithm [21] predicts about 23% helical content in aqueous solution. The helix is attributed to the mastoparan part of the peptide. Fig. 7 also shows CD spectra of transportan in 100 mM SDS, 0.1 mM DMPC and DMPG. Fig. 8 shows the CD spectra of transportan at the higher (1 mM) phospholipid concentrations. Transportan appears to have about the same amount of structure in the presence of 1 mM vesicles (DMPC, DMPG and PS) as in 100 mM SDS micelles, with around 60% helicity (Table 4). The CD spectra of transportan in the presence of DMPC vesicles were not affected by variation of the temperature, around the lipid phase transition temperature of 23°C (spectra not shown). For a more complete picture we measured the spectrum of transportan in a phospholipid mixture of DMPG and DMPC, at a 3:7 molar ratio (Fig. 8). This mixture is found to induce the same amount of structure in transportan as the neutral or negatively charged vesicles alone, again strongly suggesting that for transportan it is the hydrophobicity of the membrane mimetic environment, rather than its charge,

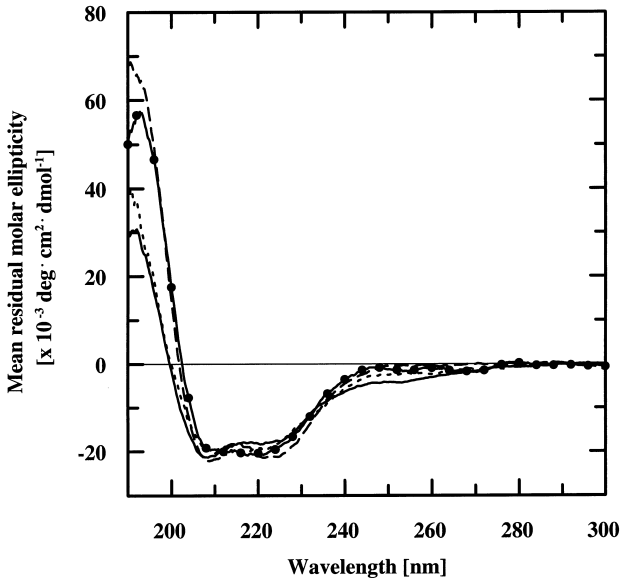

Fig. 8. CD spectra of 10 μM transportan in the presence of vesicles from 1 mM DMPG (●), 1 mM DMPC (——), 1 mM PS (- - -), and 1 mM DMPG:DMPC (3:7) (— — —) in 50 mM phosphate buffer, pH 7.0.

that dictates interaction. Reducing the phospholipid (DMPC or DMPG) concentration 10-fold to 0.1 mM still gives a significant amount of α-helix structure of about 44% in transportan, compared to 30% in water. In 30% HFP, we again obtained the maximal degree of helicity, almost 70% (spectra not shown).

4. Discussion

The pAntp peptide from the Antennapedia homeodomain is the archetypical so-called Trojan peptide [1]. Good transport properties have also been found with the new homeodomain-derived peptide, pIsl (unpublished results). In the present work, the two homeo-peptides, pAntp and pIsl, exhibited very similar behavior in terms of their interaction with, and structure induction in, membrane model systems. The results of the fluorescence spectroscopy (Table 1; Fig. 2) show that both peptides interact only with the negatively charged membrane mimetics, suggesting that it is mainly electrostatic forces that are driving in their binding to membranes. EPR results (Table 2; Figs. 3 and 4), support this observation and also shed further light on the dynamics of pAntp in the various membrane mimics. As expected, the rotational correlation time of the spin-labeled pAntp is slower in charged vesicles (DOPG and DMPG) than in SDS (by a factor of about two), but this does not reflect the difference in size between vesicles and micelles. This means that with the charged vesicles pAntp is only partially immobilized, and that the peptide (or at least its spin-labeled N-terminal moiety) still retains significant rotational freedom independent of the vesicle.

From CD spectroscopy (Table 3; Figs. 5 and 6) we can see that while the two homeo-peptides assume a predominantly random coil structure in aqueous solution, they both also contain a significant antiparallel β-sheet contribution (42% and 33% for pAntp and pIsl, respectively). This result is also supported by our preliminary observations with FTIR spectroscopy on a 1 mM aqueous solution of pAntp, indicating contributions mainly from random coil and β-sheet secondary structures (spectra not shown). The β-sheet contribution increases considerably upon binding to the negatively charged (DMPG) vesicles to 66% and 56% for pAntp and pIsl, respectively (Figs. 5 and 6). An earlier study of phospholipid monolayers with surface infrared (IR) spectroscopy has also suggested that pAntp is adsorbed, preferentially, onto charged phospholipids with a high degree of β-structure (hairpin-like), parallel to the surface [22]. The amounts of β-structure calculated in the IR study are in reasonable agreement with the values obtained here. The β-sheet-like structures of the ho-

Table 4
Summary of the main CD results for transportan

Medium	$[\theta]_{222}$ (deg cm^2 dmol^{-1})	% α-helix
Buffer (pH 7)	−8 500	30
1 mM DMPC	−22 400	63
0.1 mM DMPC	−14 600	44
1 mM DMPG	−20 500	58
0.1 mM DMPG	−14 700	44
1 mM PS	−19 600	56
1 mM DMPC:DMPG (7:3)	−21 200	60
100 mM SDS	−19 500	56
HFP:H_2O (3:7)	−24 300	67

The spectra were measured at 20°C. Transportan concentration was 10 μM, in the presence of vesicles prepared with phospholipid concentrations of either 0.1 mM or 1 mM (in 50 mM phosphate buffer, pH 7.0), or 100 mM SDS (in water, pH 3). The α-helix content was calculated according to Eq. 3.

meo-peptides, free in aqueous solution as well as bound to phospholipid vesicles, are in contrast to their helical nature within the intact homeodomain proteins. A recent molecular dynamics simulation of the unfolding of the Engrailed homeodomain (61 residues and highly homologous to the Antennapedia homeodomain) indicated an unusual stability of helix III, corresponding to the homeo-peptide sequences pAntp and pIsl [23]. Whether these peptide sequences within the entire homeodomain proteins retain their helical stability during the translocation process is, however, not known.

The synthetic peptide, transportan, does not appear to differentiate between the neutral and negatively charged membrane mimics, as demonstrated by its indiscriminant binding and helical structure induction (Tables 1 and 4; Figs. 3, 7 and 8). Hence, for transportan, the hydrophobicity of the environment alone is enough to promote binding. For 10 μM transportan, 1 mM phospholipid concentration was required to induce an optimal degree of helicity.

From NMR spectroscopy the pAntp peptide was assigned an amphipathic helical structure in SDS micelles [12,13]. Transportan in SDS micelles has also been studied by NMR in order to determine the topology of the peptide [12]. It was found that only its mastoparan part is embedded in the micelle with a helical structure, with the galanin part lying on the surface of the micelle. Our fluorescence results show that the Trp moiety of transportan is only partially protected in SDS micelles, and are therefore in agreement with the NMR results [12]. This Trp moiety is protected to the same degree, irrespective of the type of membrane mimic, a reflection of the indiscriminant binding of transportan. With DMPG and DOPG vesicles the quenching constants (Table 1) suggest that the Trp fluorophores of the homeo-peptides are less exposed than Trp of transportan to the classic hydrophilic quencher, acrylamide. The wavelength shift of the fluorescence emission, on the other hand, is almost the same for the homeo-peptides as for transportan, suggesting that the Trp residues in all three peptides reside in an environment of similar polarity. Recently neutron reflectivity was applied in order to locate the pAntp molecule with phospholipid deposits [24]. The low resolution only allowed localization of peptide particles within the head group region of the membrane.

The difficulty to observe peptide structure in the presence of phospholipid vesicles at the higher lipid concentrations underlines the problems of using far-UV CD with vesicles. However, when dealing with a strong signal, as in the case of the well-defined α-helices of transportan, the problem is manageable. Composite CD spectra with a β-structure component, on the other hand, are far more challenging. To improve the observations of the weak signals, the light scattering was minimized through 10-fold reduction of the phospholipid concentration, so that a significant CD signal indicating structure induction could be observed. We also have to bear in mind that the CD contributions of the Trp side chains can obscure precise quantitation of molar ellipticities in peptides [25].

With SDS micelles the problems with CD light scattering are mostly avoided. Micelles have been extensively used as membrane mimetics, particularly in NMR studies [26]. SDS micelles have the limitation of small size and high curvature, which may affect the nature of their interaction with peptides. With transportan all the membrane mimetics, SDS micelles included, stabilize approximately the same amount of secondary structure, with a dominating α-helix component. In contrast, the two homeo-peptides, pAntp and pIsl, behave differently in the presence of SDS micelles as opposed to vesicles. Whereas SDS induces a helical structure, the negatively charged vesicles stabilize a significant degree of β-structure. Therefore, it is clear that results with SDS micelles on secondary structures should be extrapolated only with caution. As membrane models, phospholipid vesicles are far more realistic.

The design of a minimal primary sequence for a peptide with optimal cell penetration properties is not straightforward. A number of positively charged residues are needed, but no unique amino acid is responsible. Truncated pAntp analogues retain some function, but the C-terminal segment (52–58) was reported to be necessary [27]. Also, with transportan, its C-terminal segment was important. However, with six residues truncated at the N-terminal the 21-mer was still functioning as a vector [28].

The translocation of pAntp, labeled with a fluorescence probe, has been followed by microscopy in a model system [29]. The results suggest that only the interaction of the peptide with the membrane lipids is

involved in the uptake and that no pore formation is required. The internalization of transport peptides in cellular systems has been stated to be energy independent [8]. This probably means that no coupled (mediated) transport takes place. Without the presence of a transmembrane potential, it is difficult to imagine an effective translocation for any transport peptide. In order to explain the internalization of the pAntp molecule, and its cargo, a model based on a destabilization of the bilayer by the formation of some inverted micelles has been put forward [1,5,7,8]. In the case of antimicrobial peptides with translocation properties, it has been reported that magainin 2 functions via transient pore formation and lipid flip-flop with lytic activity [30]. In contrast, buforin 2 exhibits an efficient translocation without significant membrane permeabilization or lipid flip-flop [31]. These studies were carried out with a diffusion potential present.

It is the peptide-membrane interactions, and their underlying physico-chemical processes, which should define the translocating properties of the transport peptides, hence dictating the entire mechanism of entry for each of these peptides. Whereas the interaction of the peptides with the membrane is of fundamental importance, it was up to now unclear whether a specific type of peptide conformation was mandatory for efficient membrane translocation. Evidence from an earlier study, in which substituting one or three amino acids with prolines did not alter the pAntp internalization strongly [7], suggested that this is not the case. A similar conclusion was reached in a recent study on purely synthetic transporting peptides, with different degrees of helicity (amphipathicity) [32]. It has recently been suggested, from molecular modeling, that penetratin and transportan may enter cells by different mechanisms [33]. The present study demonstrates that the peptide-membrane interactions induce different types of stable secondary structures in different transport peptides. We, therefore, conclude that the nature of the stable secondary structures induced by the biomembrane model systems is not directly correlated with a common transport property of the peptides.

Acknowledgements

We would like to thank Torbjörn Astlind for expert assistance with the spectroscopic experiments and Martina Lindqvist for expert help with the preliminary FTIR measurement. This study was supported by grants from the Swedish Natural Science Research Council and from the EU program contract No. MAS3-CT97-0156.

References

[1] D. Derossi, G. Chassaing, A. Prochiantz, Trends Cell Biol. 8 (1998) 84–87.
[2] M. Lindgren, M. Hällbrink, A. Prochiantz, Ü. Langel, Trends Pharmacol. Sci. 21 (2000) 99–103.
[3] M. Pooga, U. Soomets, M. Hällbrink, A. Valkna, K. Saar, K. Rezaei, U. Kahl, J.-X. Hao, X.-J. Xu, Z. Wiesenfeld-Hallin, T. Hökfelt, T. Bartfai, Ü. Langel, Nat. Biotechnol. 16 (1998) 857–861.
[4] J. Brugidou, C. Legrand, J. Mery, A. Rabie, Biochem. Biophys. Res. Commun. 214 (1995) 685–693.
[5] A. Prochiantz, Hum. Psychopharmacol. Clin. Exp. 14 (1999) S11–S15.
[6] D. Derossi, A.H. Joliot, G. Chassaing, A. Prochiantz, J. Biol. Chem. 269 (1994) 10444–10450.
[7] D. Derossi, S. Calvet, A. Trembleau, A. Brunissen, G. Chassaing, A. Prochiantz, J. Biol. Chem. 271 (1996) 18188–18193.
[8] A. Prochiantz, Ann. NY Acad. Sci. 886 (1999) 172–179.
[9] M. Pooga, M. Hällbrink, M. Zorko, Ü. Langel, FASEB J. 12 (1998) 67–77.
[10] O. Karlsson, S. Thor, T. Norberg, H. Ohlsson, T. Edlund, Nature 344 (1990) 879–882.
[11] H. Ippel, G. Larsson, G. Behravan, J. Zdunek, M. Lindqvist, J. Schleucher, P.-O. Lycksell, S. Wijmenga, J. Mol. Biol. 288 (1998) 689–703.
[12] M. Lindberg, J. Jarvet, Ü. Langel, A. Gräslund, Biochemistry 40 (2001) 3141–3149.
[13] J.-P. Berlose, O. Convert, D. Derossi, A. Brunissen, G. Chassaing, Eur. J. Biochem. 242 (1996) 372–386.
[14] B.-M. Backlund, G. Wikander, T. Peeters, A. Gräslund, Biochim. Biophys. Acta 1190 (1994) 337–344.
[15] J.R. Lakowicz, Principles of Fluorescence Spectroscopy, 2nd edn., Kluwer Academic, New York, 1999.
[16] L.E.G. Eriksson, H. Beving, Arch. Biochem. Biophys. 303 (1993) 296–301.
[17] N. Greenfield, G.D. Fasman, Biochemistry 8 (1969) 4108–4116.
[18] P. Manavalan, W.C. Johnson Jr., Anal. Biochem. 167 (1987) 76–85.
[19] B.L. Bales, L. Messina, A. Vidal, M. Peric, J. Phys. Chem. 102 (1998) 10347–10358.

[20] J. Jarvet, J. Zdunek, P. Damberg, A. Gräslund, Biochemistry 36 (1997) 8153–8163.
[21] V. Muñoz, L. Serrano, Biopolymers 41 (1997) 495–509.
[22] E. Bellet-Amalric, D. Blaudez, B. Desbat, F. Graner, F. Gauthier, A. Renault, Biochim. Biophys. Acta 1467 (2000) 131–143.
[23] U. Mayor, C.M. Johnson, V. Dagett, A.R. Fersht, Proc. Natl. Acad. Sci. USA 97 (2000) 13518–13522.
[24] G. Fragneto, F. Graner, T. Charitat, P. Dubos, E. Bellet-Amalric, Langmuir 16 (2000) 4581–4588.
[25] A. Chakrabartty, T. Kortemme, S. Padmanabhan, R.L. Baldwin, Biochemistry 32 (1993) 5560–5565.
[26] P. Damberg, J. Jarvet, A. Gräslund, Methods Enzymol. 339 (2001) 271–285.
[27] P.M. Fischer, N.Z. Zhelev, S. Wang, J.E. Melville, R. Fåhraeus, D.P. Lane, J. Pept. Res. 55 (2000) 163–172.
[28] U. Soomets, M. Lindgren, X. Gallet, M. Hällbrink, A. Elmquist, L. Balaspiri, M. Zorko, M. Pooga, R. Brasseur, Ü. Langel, Biochim. Biophys. Acta 1467 (2000) 165–176.
[29] P. Thorén, D. Persson, M. Karlsson, B. Nordén, FEBS Lett. 482 (2000) 265–268.
[30] K. Matsuzaki, Biochim. Biophys. Acta 1376 (1998) 391–400.
[31] S. Kobayashi, K. Takeshima, C.B. Park, S.C. Kim, K. Matsuzaki, Biochemistry 39 (2000) 8648–8654.
[32] A. Scheller, B. Wiesner, M. Melzig, M. Bienert, J. Oehlke, Eur. J. Biochem. 267 (2000) 6043–6049.
[33] M. Lindgren, X. Gallet, U. Soomets, M. Hällbrink, E. Bråkenhielm, M. Pooga, R. Brasseur, Ü. Langel, Bioconjugate Chem. 11 (2000) 619–626.